

A Neural-Network-Based Model Predictive Control of Three-Phase Inverter With an Output LC Filter

Ihab S. Mohamed*, Stefano Rovetta†, Ahmed A. Zaki Diab ‡, and Ton Duc Do §

*INRIA Sophia Antipolis - Méditerranée, University Côte d'Azur, France

†Department of Informatics, Bioengineering, Robotics and Systems Engineering, University of Genoa, Italy

‡ Electrical Engineering Department, Faculty of Engineering, Minia University, Egypt

§ Department of Robotics and Mechatronics, School of Science and Technology (SST), Nazarbayev University, Astana Z05H0P9, Republic of Kazakhstan

Abstract—Model predictive control (MPC) has become one of the well-established modern control methods for three-phase inverters with an output LC filter, where a high-quality voltage with low total harmonic distortion (THD) is needed. Though it is an intuitive controller easy to understand and implement, it has the significant disadvantage of requiring a large number of online calculations for solving the optimization problem. On the other hand, the application of model-free approaches such as artificial neural network-based (ANN-based) approaches is currently growing rapidly in the area of power electronics and drives. This paper presents a new control scheme for a two-level converter based on combining MPC with feed-forward ANN, with the aim of getting lower THD and improving the steady and dynamic performance of the system for different types of loads. First, MPC is used, as an expert, in the training phase to generate data required for training the proposed neural network. Then, once the neural network is fine-tuned, it can be successfully used online for voltage tracking purpose, without the need of using MPC. The proposed ANN-based control strategy is validated through simulation, using MATLAB/Simulink tools, taking into account different loads conditions. Moreover, the performance of the ANN-based controller is evaluated, on several samples of linear and non-linear loads under various operating conditions, and compared to that of MPC, demonstrating the excellent steady-state and dynamic performance of the proposed ANN-based control strategy.

Index Terms—Three-phase inverter, model predictive control, artificial neural network, UPS systems.

I. INTRODUCTION

The three-phase inverter is an extensively popular device, which is commonly used for transferring energy from a DC voltage source to an AC load. The control of three-phase inverters has received much attention in the last decades both in the scientific literature and in the industry-oriented research [1], [2]. In particular, for applications such as uninterruptible power supplies (UPSs), energy-storage systems, variable frequency drives, and distributed generation, the inverters are commonly used with an output LC filter to provide a high-quality sinusoidal output voltage with low total harmonic distortion (THD) for various types of loads, especially for unbalanced or nonlinear loads [3]–[7]. However, the performance of the inverter is mainly dependent on the applied control technique. These controllers must cope with the load variations, the non-linearity of the system, and ensuring stability under any operating condition with a fast transient response [8].

In the literature, various types of classical and modern control schemes have been studied and proposed in order to improve the performance of the converters, such as non-linear methods (e.g., hysteresis voltage control (HVC)) [9], linear methods (e.g., proportional-integral (PI) controller with pulse-width modulation (PWM) and space vector modulation (SVM)) [10]–[13], multi-loop feedback control [14], [15], deadbeat control [16]–[20], repetitive-based controllers [21], [22], linear quadratic controller (LQR) [23], and sliding-mode control [24], [25]. Most of these control schemes, in a way or another, are characterized by a number of limitations.

Just to name a few, the major drawback of non-linear methods (e.g., HVC), which require high switching frequency for effective operation, is having a variable switching frequency which creates resonance problems which reduce the converter's efficiency [26], [27]. On the other hand, although the linear methods, which require carrier-based modulators, have the advantage of constant switching frequency, their dynamic response is weak comparing with HVC, because of the slow response of the modulator. However, both linear and nonlinear methods are extensively used for generating the switching signals of the inverter because of the simplicity of the controller implementation. Another example is deadbeat control which provides fast transient response, however, it has high sensitivity to model uncertainties, measurement noise, and parameter perturbations, in particular for high sampling rates. Other modern control approaches based on H_∞ control theory [28] and μ synthesis [29] have been proposed, with the aim of handling the possible uncertainties in the system.

Model predictive control (MPC) has become one of the well-established modern control methods in power electronics, particularly for three-phase inverters with LC filter according to [1], [26], [30]–[32]. The key characteristic of MPC is to explicitly use the model of the system to predict the future behavior of the variables to be controlled, considering a certain time horizon. Afterwards, MPC selects the optimal control action (i.e., optimal switching signals) based on the minimization of a pre-defined cost function, which represents the desired behavior of the system [33]–[35]. The main features of MPC can be summarized as: (i) an intuitive controller easy to understand and implement, with a fast dynamic response; (ii) the simple inclusion of system constraints and nonlinearities, and multivariable cases; (iii) the flexibility to include other

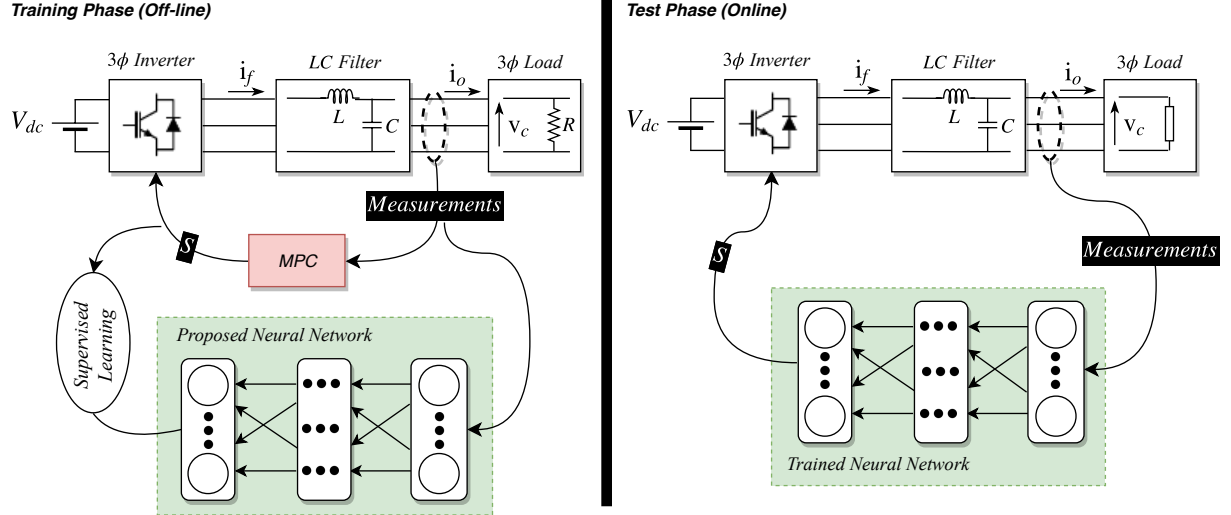


Fig. 1. An overview of the proposed control strategy: the training phase combines between using MPC for predicting the output voltage of the inverter and collecting data, under full-state observation, for training the neural network proposed. In the test phase, the trained neural network is employed online to control the output voltage of the inverter instead of MPC, considering linear and non-linear loads.

system requirements. On the other hand, a major drawback of MPC is that it requires the optimization problem to be solved online, which involves a huge amount of real-time calculations. However, different solutions have been introduced in order to address this problem, as proposed in [31], [36], [37].

On the other hand, the application of data-driven methodologies (or model-free approaches, particularly artificial neural networks ANNs-based approaches) is currently growing rapidly in the area of power electronics and drives. These can be used for describing the behavior of the complex systems [38]. In particular, ANN-based controllers and estimators have been widely used in identification and control of power converters and motor drives [39]. As an example, they can be used to estimate the rotor speed, rotor-flux, and torque of induction motors [40]–[42], in addition to the identification and estimation of the stator current of induction motor drives [43]. Moreover, several ANN-based methods have been used in control of power converters, as presented in [44]–[47]. Indeed, the ANN-based controllers have some advantages compared to other control methods such as: (i) their design does not require the mathematical model of the system to be controlled, considering the whole system as a black-box; (ii) they can generally improve the performance of the system when they are properly tuned; (iii) they are usually easier to be tuned as compared to conventional controllers; (iv) they can be designed based on the data acquired from a real system or a plant in the absence of necessary expert knowledge. But, they require a large number of training data. However, as the present work suggests, this is not a major drawback because large amounts of data can be obtained using reliable simulation tools.

By taking advantage of the flexibility of MPC at training time, this paper proposes a feed-forward ANN-based controller for a three-phase inverter with output *LC* filter for UPS applications, with the aim of getting lower THD and good performance for different types of loads. The proposed controller

undergoes two main steps: (i) the use of MPC as an expert or a teacher for generating the data required for training off-line the proposed neural network using standard supervised learning, under full-state observation of the system; (ii) once the off-line training is performed, the trained ANN can successfully control the output voltage of the inverter, without the need of using MPC at test time, as illustrated in Fig. 1. A performance comparison between the proposed ANN-based approach and the conventional MPC, under various operating conditions, is studied. To the best of our knowledge, the control of a three-phase inverter with an output *LC* filter using a feed-forward ANN-based MPC has not been reported in the literature.

The rest of the paper is organized as follows. Section II deals with the mathematical model of the three-phase voltage-source inverter with *LC* filter, whereas in Section III the proposed predictive controller strategy is explained. The ANN-based control scheme proposed in this paper is described in Section IV. In Section V, simulation implementation and results are discussed for both proposed control schemes, then the conclusion is provided in Section VI.

II. SYSTEM DESCRIPTION AND MODELING

A. System description via Clarke transformation

The power circuit of the three-phase voltage-source inverter considered in this paper is depicted in Fig. 2. In the present case, the load is assumed to be unknown, while the models of the converter and filter are presented [30]. Moreover, the two switches of each leg of the converter operate in a complementary mode, in order to avoid the occurrence of short-circuit conditions. Thus, the switching states of the converter can be represented by the three binary switching signals, S_a , S_b , and S_c , as follows:

$$S_a = \begin{cases} 1, & \text{if } S_1 \text{ ON and } S_4 \text{ OFF} \\ 0, & \text{if } S_1 \text{ OFF and } S_4 \text{ ON} \end{cases}$$

$$S_b = \begin{cases} 1, & \text{if } S_2 \text{ ON and } S_5 \text{ OFF} \\ 0, & \text{if } S_2 \text{ OFF and } S_5 \text{ ON} \end{cases}$$

$$S_c = \begin{cases} 1, & \text{if } S_3 \text{ ON and } S_6 \text{ OFF} \\ 0, & \text{if } S_3 \text{ OFF and } S_6 \text{ ON} \end{cases}$$

These switching states can be expressed in vectorial form (i.e., in $\alpha\beta$ reference frame) by following transformation:

$$\begin{aligned} S &= \frac{2}{3}(S_a + aS_b + a^2S_c) \equiv S_\alpha + jS_\beta, \\ \begin{bmatrix} S_\alpha \\ S_\beta \end{bmatrix} &= \frac{2}{3} \begin{bmatrix} 1 & -1/2 & -1/2 \\ 0 & \sqrt{3}/2 & -\sqrt{3}/2 \end{bmatrix} \begin{bmatrix} S_a \\ S_b \\ S_c \end{bmatrix}, \end{aligned} \quad (1)$$

$\underbrace{S}_{=:T_c \text{ (Clarke transformation)}} \quad \underbrace{S_{abc}}_{S_{abc}}$

where $a = e^{j(2\pi/3)}$. It is noteworthy that the switching devices are assumed to be ideal switches, therefore the process of switching-ON/-OFF is not taken into consideration [32].

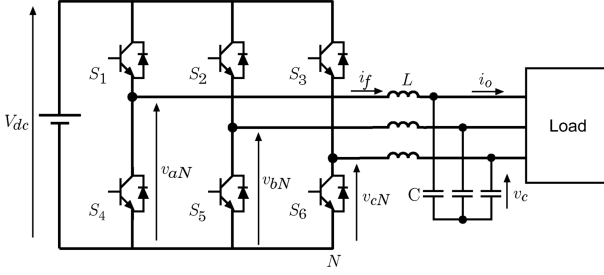


Fig. 2. Three-phase voltage-source inverter with an output LC filter.

The possible output-voltage space vectors generated by the inverter can be obtained by

$$v_i = \frac{2}{3}(v_{aN} + av_{BN} + a^2v_{CN}) \quad (2)$$

where v_{aN} , v_{BN} , and v_{CN} represent the phase-to-neutral, N , voltages of the inverter. On the other hand, the voltage vector v_i can be defined, in terms of the switching state vector S and the dc-link voltage V_{dc} , by

$$v_i = V_{dc}S. \quad (3)$$

Fig. 3 illustrates the eight switching states and, consequently, the eight voltage vectors generated by the inverter using (1) and (3), considering all the possible combinations of the switching signals S_a , S_b , and S_c . It is noteworthy that only seven different voltage vectors are considered as possible outputs, since $v_0 = v_7$.

Similarly, as in (1), the filter current i_f , the output voltage v_c , and the output current i_o can be expressed in the vectorial form as

$$i_f = \frac{2}{3}(i_{fa} + ai_{fb} + a^2i_{fc}) \equiv i_{f\alpha} + j i_{f\beta}, \quad (4)$$

$$v_c = \frac{2}{3}(v_{ca} + av_{cb} + a^2v_{cc}) \equiv v_{c\alpha} + j v_{c\beta}, \quad (5)$$

$$i_o = \frac{2}{3}(i_{oa} + ai_{ob} + a^2i_{oc}) \equiv i_{o\alpha} + j i_{o\beta}. \quad (6)$$

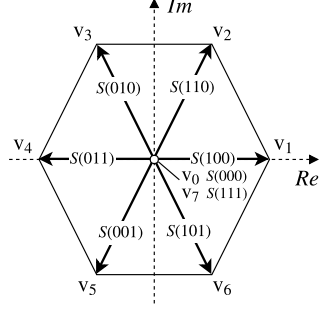


Fig. 3. Eight possible combinations of the gating signals, and their corresponding voltage vectors generated by the inverter in the complex plane.

B. *LC* filter modeling

As far as the model of LC filter is concerned, it can be described by two equations, the former describes the inductance dynamics, whereas the latter describing the capacitor dynamics [1]. These two equations can be written as a continuous-time state-space system as

$$\begin{aligned} \frac{dx}{dt} &= Ax + Bv_i + B_qi_o, \\ \frac{d}{dt} \begin{bmatrix} i_f \\ v_c \end{bmatrix} &= \underbrace{\begin{bmatrix} 0 & -\frac{1}{L} \\ \frac{1}{C} & 0 \end{bmatrix}}_A \underbrace{\begin{bmatrix} i_f \\ v_c \end{bmatrix}}_x + \underbrace{\begin{bmatrix} \frac{1}{L} \\ 0 \end{bmatrix}}_B v_i + \underbrace{\begin{bmatrix} 0 \\ -\frac{1}{C} \end{bmatrix}}_{B_q} i_o, \end{aligned} \quad (7)$$

where L and C are the filter inductance and the filter capacitance, respectively. The output voltage v_c and the filter current i_f can be measured, whilst the voltage vector v_i can be calculated using (3). The output current i_o is considered as a disturbance due to its dependence on an unknown load, whereas the value of V_{dc} is assumed to be fixed and known. The output voltage v_c is considered as the output of the system, which can be written as a state equation as $v_c = [0 \ 1] x$.

Then, using (7), the discrete-time state-space model of the filter can be obtained for a sampling time T_s as

$$x(k+1) = A_q x(k) + B_q v_i(k) + B_{dq} i_o(k),$$

$$\begin{aligned} \underbrace{\begin{bmatrix} i_f(k+1) \\ v_c(k+1) \end{bmatrix}}_{x(k+1)} &= \underbrace{e^{AT_s}}_{A_q} \underbrace{\begin{bmatrix} i_f(k) \\ v_c(k) \end{bmatrix}}_{x(k)} + \int_0^{T_s} \underbrace{e^{A\tau} B d\tau}_{B_q} v_i(k) \\ &+ \int_0^{T_s} \underbrace{e^{A\tau} B_d d\tau}_{B_{dq}} i_o(k). \end{aligned} \quad (8)$$

This model is used by the predictive controller (i.e., MPC) to predict the output voltage v_c for all given input voltage vector v_i . Then, for predicting the output voltage v_c using (8), the output current i_o is needed and can be estimated using (9), assuming that $i_o(k-1) = i_o(k)$ for sufficiently small sampling times T_s as proposed in [1], [35].

$$i_o(k-1) \cong i_o(k) = i_f(k-1) - \frac{C}{T_s} (v_c(k) - v_c(k-1)) \quad (9)$$

III. MODEL PREDICTIVE CONTROL FOR NEURAL NETWORK

In this paper, the model predictive control (MPC) proposed in [30], and which provides the state-of-art of output-voltage control of three-phase inverter for UPS applications, has been used: (i) to generate the data required for the off-line training of the proposed neural network, and (ii) to compare its performance with the proposed ANN-based controller under linear and non-linear load conditions.

A. Proposed Predictive Controller Strategy

In the proposed control strategy, it has been assumed that the inverter generates only a finite number of possible switching states and their corresponding output-voltage vectors, making it possible to solve the optimization problem of the predictive controller online [1]. MPC exploits the discrete-time model of the inverter to predict the future behavior of the variables to be controlled, for each switching state. Thereafter, the optimum switching state is selected, based on the minimization of a pre-defined cost function, and directly fed to the power switches of the converter in each sampling interval T_s , without the need for a modulation stage. The cost function to be minimized has been chosen in order to achieve the lowest error between the predicted output voltage and the reference voltage. In this work, a cost function J which defines the desired behavior of the system is expressed in orthogonal coordinates by

$$J = \left(\mathbf{v}_{c\alpha}^* - \mathbf{v}_{c\alpha}(k+1) \right)^2 + \left(\mathbf{v}_{c\beta}^* - \mathbf{v}_{c\beta}(k+1) \right)^2 \quad (10)$$

where $\mathbf{v}_{c\alpha}^*$ and $\mathbf{v}_{c\beta}^*$ are the real and imaginary parts of the output-voltage reference vector \mathbf{v}_c^* , while $\mathbf{v}_{c\alpha}$ and $\mathbf{v}_{c\beta}$ are the real and imaginary parts of the predicted output-voltage vector $\mathbf{v}_c(k+1)$.

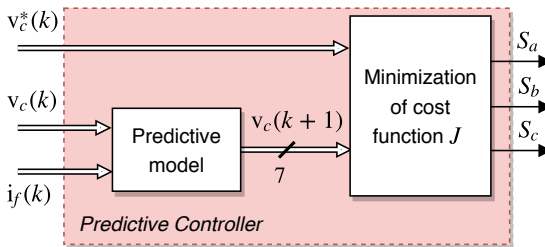


Fig. 4. Schematic diagram of output voltage control of a three-phase inverter with an output LC filter using MPC.

The block diagram of MPC, considering only one-step prediction horizon, for a three-phase inverter with output LC filter is shown in Fig. 4. The control cycle of the predictive controller at sampling instant k is described as a pseudo code in Algorithm 1 with more detail. Line 1 of the code declares the control function, where the switching signals S_a , S_b , and S_c are the outputs, while the inputs are the measured variables of the filter current $i_f(k)$, the output voltage $v_c(k)$, and the reference voltage $v_c^*(k)$ at sampling time k , all expressed in $\alpha\beta$ coordinates. The two variables, $i_f(k-1)$ and $v_c(k-1)$, are recalled from the previous sampling instant (lines 7 to 9),

which are firstly initialized for $k = 1$ (lines 3 to 6). These two variables are used to estimate the output current $i_o(k)$ given by (9) (line 10), in order to obtain the possible predictions of $v_c(k+1)$ using (8).

The optimization problem to be solved is performed between lines 12 and 20. The code sequentially selects one of the seven possible voltage vectors v_i generated by the inverter based on (3) (line 13) and applies it, in order to obtain the output voltage prediction $v_c(k+1)$ at instant $k+1$, as in line 14. The cost function given by (10) is used to evaluate the error between the reference and the predicted output voltage at instant $k+1$ for each voltage vector (line 15). The code selects the *optimal* value of the cost function J_{opt} , and the *optimum* voltage vector x_{opt} is then chosen (lines 16 to 19). Note that, J_{opt} is initialized with a very high value (line 11). Finally, the switching states, S_a , S_b , and S_c , corresponding to the *optimum* voltage vector are generated and applied at the next sampling instant, as illustrated in Fig. 3 (line 22).

Algorithm 1 Pseudo code of the proposed MPC

```

1: function  $[S_a, S_b, S_c] = MPC(i_f(k), v_c(k), v_c^*(k))$ 
2:   Measure the first sampled values as  $i_f(1)$ ,  $v_c(1)$ ,  $v_c^*(1)$ ;
3:   if  $k = 1$  then
4:     Set  $i_f(k-1) = i_f(0) = 0 + j0$ ;
5:     Set  $v_c(k-1) = v_c(0) = 0 + j0$ ;
6:   end if
7:   if  $k > 1$  then
8:     Recall the measured variables  $i_f(k-1)$ ,  $v_c(k-1)$ ;
9:   end if
10:  Estimate  $i_o(k) = i_f(k-1) - \frac{C}{T_s} (v_c(k) - v_c(k-1))$ ;
11:  Set  $J_{opt} = \infty$ ;
12:  for  $l = 1$  to  $7$  do
13:    Compute  $v_i(l) = S(l)V_{dc}$ ;
14:    Predict  $v_c(k+1)$  at instant  $k+1$  using (8);
15:    Evaluate  $J = \left( v_c^*(k) - v_c(k+1) \right)^2$ ;
16:    if  $J(l) < J_{opt}$  then
17:      Set  $J_{opt} = J(l)$ ;
18:      Set  $x_{opt} = l$ ;
19:    end if
20:  end for
21:  Set  $S_{opt} = S(x_{opt})$ ;
22:  return  $[S_a, S_b, S_c] = [S_{opt}(1), S_{opt}(2), S_{opt}(3)]$ ;
23: end function

```

B. Discussion

In fact, all the control approaches proposed in the literature, in a way or another, are model-based approaches, which require in general either diverse computational or approximative procedures for applying their solution. In this context, MPC, the widely used approach for three-phase inverters, relies on solving an optimization problem online, leading to a large

number of online computations. In other words, the control signal of MPC is determined by minimizing a cost function online at each time instant. The alternative approach to be considered in the present work is to apply neural network-based function approximators, which can be trained off-line to represent the optimal control law. Such an approach is expected to avoid the drawbacks associated with MPC-based control approaches, does not require the mathematical model of the system to be controlled, does not evaluate a cost function online at each sampling time, and, therefore, does not rely on an optimization problem to be solved online. For this reason, this paper focuses on the control of a three-phase inverter with output LC filter using an ANN-based approach.

IV. IMPLEMENTATION OF ANN-BASED CONTROLLER

A. Proposed Neural Network Architecture

Machine learning, and in particular artificial neural networks, is one key technology in modern control systems. An artificial neural network is an extremely flexible computational model that can be optimized to learn input-to-output mappings based on historical data. Although the most recent developments have focused on larger and larger scale problems (deep learning), improved techniques have also been proposed to improve the reliability of networks of smaller size. The result is a sound and flexible technology.

An artificial neural network (ANN) is composed of a number of simple computing elements organized in layers and linked by weighted connections. Feed-forward networks do not contain loops, so they have a static behavior and can be used to implement memoryless input-to-output mappings. In a feed-forward network it is possible to distinguish one input layer, one output layer, and hidden layers that connect the input to the output.

In this work, a feed-forward neural network (fully connected multi-layer perceptron) of the “shallow” type, i.e., one hidden layer, was used to implement the control model. A grid search tuning procedure allowed the selection of a configuration with 15 units in the hidden layer, while the number of input and output units is constrained by the number of input and output variables, respectively. Training was done via the Scaled Conjugate Gradient method [48], which exploits the good convergence properties of conjugate gradient optimization [49] and has the computational advantage of not requiring a line search, nor any user-selected parameters.

B. ANN Training Procedure

The ANN takes as inputs the measured variables of the filter current i_f , the output voltage v_c , the output current i_o , and the reference voltage v_c^* all expressed in $\alpha\beta$ coordinates. For simplicity’s sake, the real and imaginary parts of these variables are separately fed to the neural network, bringing the total number of input features to eight. On the other hand, the *optimum* voltage vector x_{opt} to be applied at each sampling instant constitute the output of the ANN. In fact, the size of the output layer is an array with a length of 7, which represents the indexes of the seven possible voltage vectors v_i that inverter generates. The output is one-hot encoded, meaning that at each

sampling instant only the index of the *optimum* voltage vector will be active (i.e., having a value of one), while others will be equal to zero.

The training data, which have been collected by MPC, comprises 70 samples, which are divided into 60 samples for specific resistive loads (i.e., for only $R = 1, 3, 5, 7, 10, 15, 20, 25, 30$, and 35Ω), whereas only 10 samples represent the case where the inverter is directly fed a non-linear load (i.e., diode-bridge rectifier) with different values of R_{NL} and C_{NL} . For each sample, the simulation is run, using MPC, under various operating conditions such as sampling time T_s , filter capacitor C , filter inductance L , DC-link voltage V_{dc} , and reference voltage v_c^* . Then, the input features of the neural network and their targets are stored for training.

For further detailed information about the MPC simulations and training samples that have been used for training the proposed ANN, please refer to:

<https://github.com/IhabMohamed/MPC-3-Phase-Inverters>

C. ANN-Based Controller

As previously mentioned, the ANN-based controller is trained off-line from samples collected via MPC, as shown in Fig. 1. After fine-tuning the ANN, the trained ANN can be used instead of MPC to control the system presented in Fig. 2.

Fig. 5 depicts the proposed block diagram of the ANN-based controller for a three-phase inverter with output LC filter, in order to generate a high-quality sinusoidal output voltage with low THD, considering different types of loads.

The control strategy of the proposed ANN-based controller at sampling time k can be described as follows:

- 1) measure the value of the filter current $i_f(k)$, the output voltage $v_c(k)$, and the output current $i_o(k)$ at sampling time k . Note that, the output current $i_o(k)$ is considered to be a measurable value, without estimation based on (9) or using the observer as in [1];
- 2) then, these measured values in addition to the reference voltage $v_c^*(k)$ are used by the trained ANN in order to explicitly generate the *optimum* voltage vector x_{opt} to be applied at instant $k + 1$;
- 3) finally, the switching states, S_a , S_b , and S_c , corresponding to the optimum voltage vector x_{opt} are applied and directly given to the power switches of the converter each sampling interval T_s .

V. SIMULATION IMPLEMENTATION AND RESULTS

A. Simulation Setup

The Simulink model and the simulations of the system shown in Fig. 2 have been implemented using MATLAB (R2018a)/Simulink software components, which runs on Ubuntu 16.04 64 bit, in order to verify the proposed ANN-based control strategy and compare its performance with the conventional predictive controller (i.e., MPC). A lower-end PC has been used for acquiring the training samples, off-line training, and online voltage tracking purpose using the proposed ANN approach. In particular, it is equipped with an Intel® Core i5-4210U 1.70 GHz CPU, 6 GB of RAM, and an Nvidia Geforce® GPU, and runs Ubuntu 16.04 64 bit.

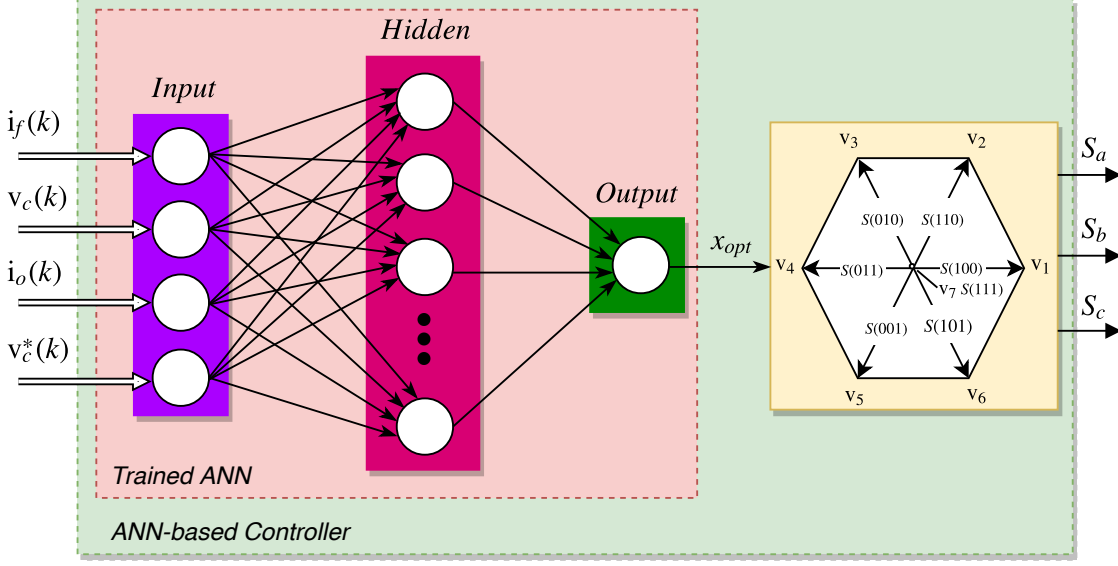


Fig. 5. Schematic diagram of output voltage control of a three-phase inverter with an output LC filter using ANN-based controller.

B. Simulation Results

The simulation of the three-phase inverter system shown in Fig. 2 was carried out, considering linear (i.e., resistive) and non-linear loads, in order to evaluate the behavior of the proposed ANN-based control strategy and compare its performance with that of MPC proposed in Section III. In particular, the steady and dynamic performance of both control strategies are studied and evaluated, taking into account different loads conditions. The parameters of the system are listed in Table I.

Table I
SYSTEM PARAMETERS

Parameter	Value
DC-link voltage V_{dc}	500 [V]
Filter capacitor C	40 [μ F]
Filter inductance L	2 [mH]
Sampling time T_s	30 [μ s]

The behavior of the ANN-based controller in steady-state operation for a resistive load of $5\text{ k}\Omega$ shown in Fig. 6, while the behavior of the predictive controller for the same resistive load is shown in Fig. 7. It is noteworthy that the amplitude and the fundamental frequency of reference voltage v_c^* are set to 200 V and 50 Hz, respectively. It can be seen in the figures that the output voltages v_c for the proposed control strategies are sinusoidal with low distortion, particularly for the ANN-based approach which has a THD of only 1.6% compared to 3.95% for MPC. Moreover, it is observed, due to the resistive load, that the output current i_o is proportional to the output voltage, whilst the filter current i_o measured at the output of the converter shows high-frequency harmonics, especially in the case of MPC, which are attenuated by the LC filter.

The transient response of both the control strategies for no-load (i.e., open-circuit) is shown in Fig. 8 and Fig. 9. Here, the filter capacitor C and filter inductance L are set to $50\text{ }\mu\text{F}$ and 3.5 mH , respectively, whilst the sampling time T_s is kept constant at a value of $30\text{ }\mu\text{s}$. It can be seen that the ANN-based

controller permits a fast and safe transient response, demonstrating the excellent dynamic performance of the proposed ANN-based control strategy. For MPC, the time elapsed in order to reach steady-state operation and to faithfully track its reference waveform is about 20 ms (1 cycle), which is affected by the change in the load, as illustrated in Table II. On the other side, for the ANN-based controller, it is observed that it takes less than 5 ms for any load, in order to reach steady-state. Furthermore, the output voltage quality of ANN-based approach is improved significantly, with a THD of 0.72% compared to 1.92% for MPC.

As previously mentioned, the proposed ANN is trained off-line using a dataset which represents only different values of resistive load under different operating conditions. However, in order to verify the feasibility and effectiveness of the proposed ANN-based controller under realistic conditions, the behavior of the system is tested online considering non-linear loads, such as a diode-bridge rectifier as shown in Fig. 10 and an inductive load. Fig. 11 and Fig. 12 show the behavior of the proposed control strategies for a diode-bridge rectifier, with values $C = 300\text{ }\mu\text{F}$ and $R = 60\text{ }\Omega$, while the behavior for an inductive load of 0.01 H is shown in Fig. 13 and Fig. 14, considering the same operating conditions presented in Table I and different amplitudes of the reference output voltage. As can be seen in the figures, the output voltage generated by the ANN-based controller outperforms that obtained using MPC for non-linear loads, despite the highly distorted output currents due to feeding a non-linear load. For instance, for MPC, the total distortion in the output voltage for the inductive load was 4.86%, while it was 2.2% for the ANN-based controller. The result of MPC can be improved by using either a smaller sampling time or a higher value of the filter capacitance [32].

In order to achieve a fair comparison and prove the superiority of the proposed ANN-based approach compared to MPC in both transient and steady-state response, Table II

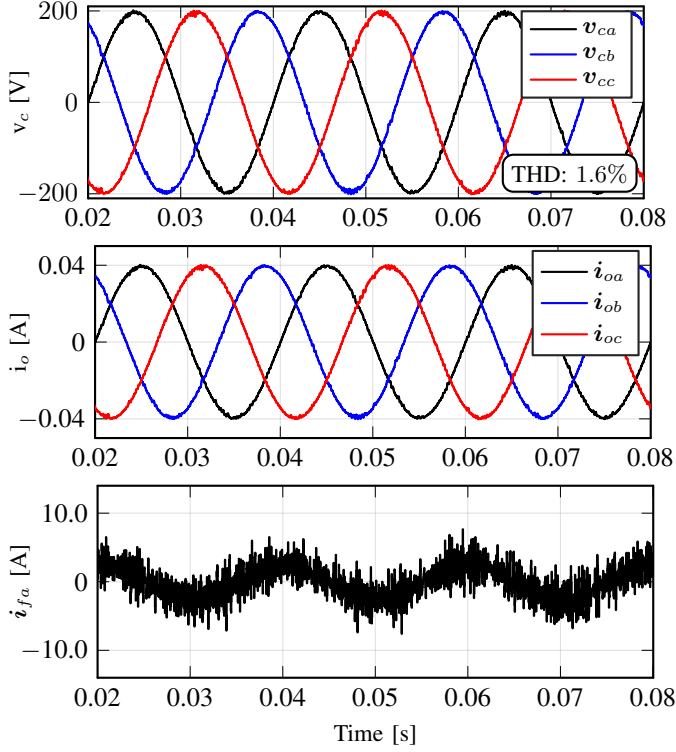


Fig. 6. Simulation results of ANN-based controller: output voltages, output currents, and filter current in steady-state for a resistive load of $5\text{ k}\Omega$.

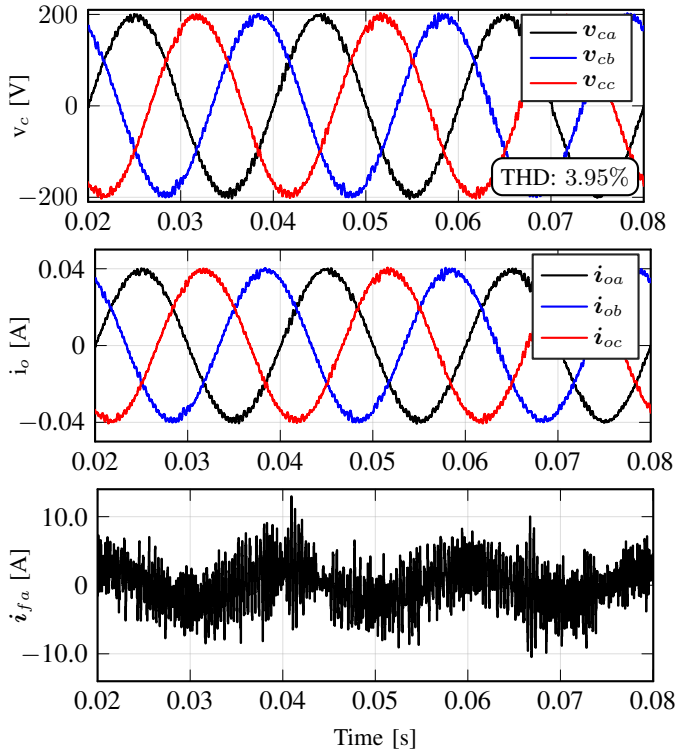


Fig. 7. Simulation results of MPC: output voltages, output currents, and filter current in steady-state for a resistive load of $5\text{ k}\Omega$.

shows a comprehensive comparison of both the control strategies for linear and non-linear loads, under various operating

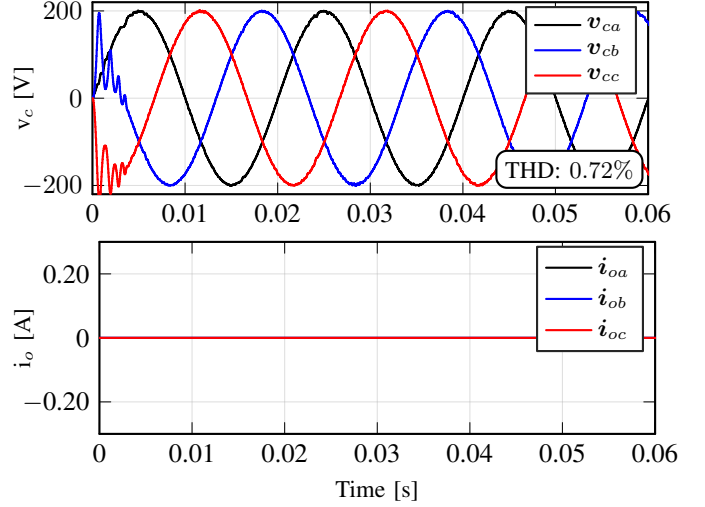


Fig. 8. Simulation results: the dynamic response of the ANN-based controller for a no-load, where the filter capacitor $C = 50\text{ }\mu\text{F}$, the filter inductance $L = 3.5\text{ mH}$, and $T_s = 30\text{ }\mu\text{s}$.

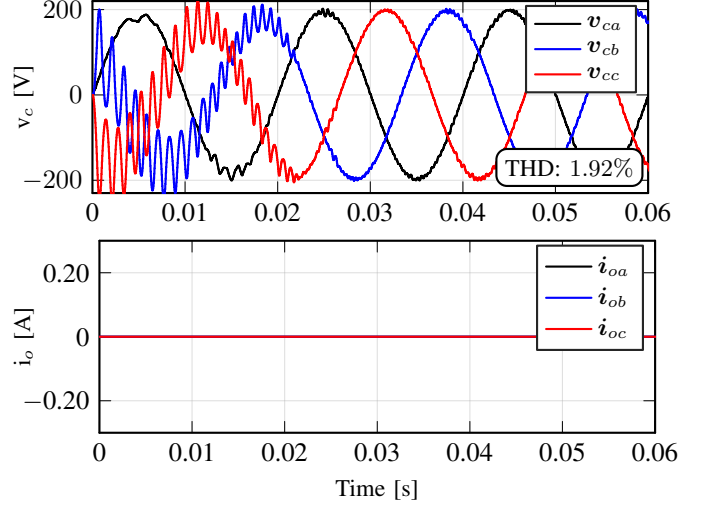


Fig. 9. Simulation results: the dynamic response of MPC for a no-load, where the filter capacitor $C = 50\text{ }\mu\text{F}$, the filter inductance $L = 3.5\text{ mH}$, and $T_s = 30\text{ }\mu\text{s}$.

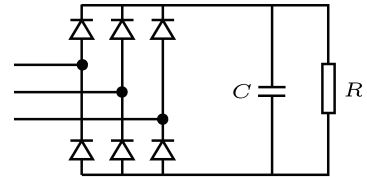


Fig. 10. Diode-bridge rectifier used as non-linear load, with values $C = 300\text{ }\mu\text{F}$ and $R = 60\text{ }\Omega$.

conditions such as sampling time T_s , filter capacitor C , filter inductance L , DC-link voltage V_{dc} , and reference voltage v_c^* . Fifty samples have been considered for testing the proposed approaches, thirty samples for different values of a resistive load, whereas the rest for a diode-bridge rectifier as a non-linear load. As anticipated, the performance of the ANN-based

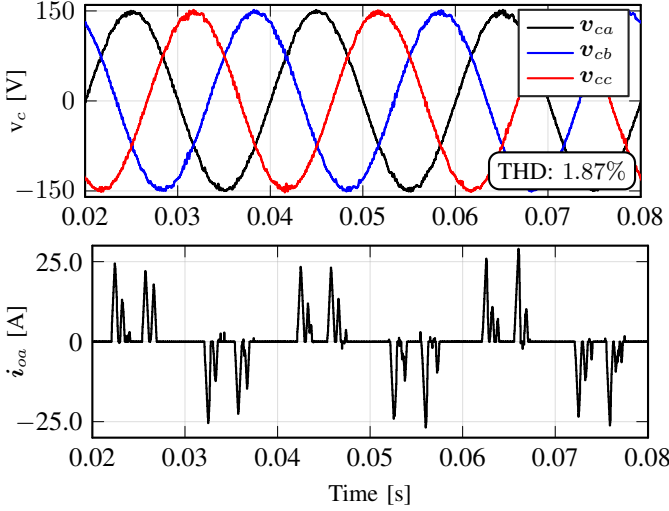


Fig. 11. Simulation results of ANN-based controller: output voltages and one-phase output current in steady-state for a diode-bridge rectifier and a reference amplitude of 150 V.

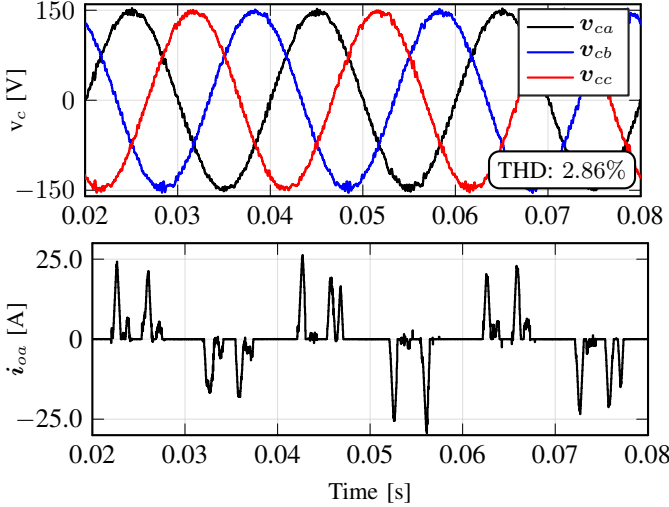


Fig. 12. Simulation results of MPC: output voltages and one-phase output current in steady-state for a diode-bridge rectifier and a reference amplitude of 150 V.

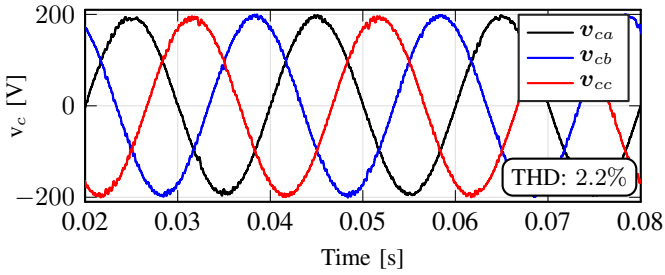


Fig. 13. Simulation results of ANN-based controller: output voltages in steady-state for an inductive load of 0.01 H and a reference amplitude of 200 V.

approach, either based on sixty or seventy training samples, outperforms that of MPC, which can be noticed in lower THD and less settling time to reach steady-state (i.e., t_{ss} , as shown

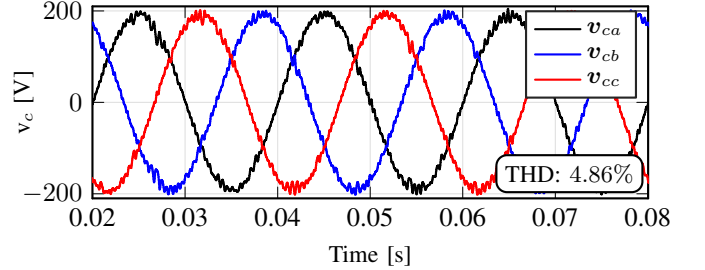


Fig. 14. Simulation results of MPC: output voltages in steady-state for an inductive load of 0.01 H and a reference amplitude of 200 V.

in the first ten samples (i.e., $S_1 - S_{10}$)). It can be noticed that the performance of the ANN-based controller using only sixty training samples is similar to that based on seventy samples (see column 8 and 9 in Table II).

However, for samples $S_{26} - S_{30}$, the output voltages obtained using MPC are better than that obtained using the ANN-based controller. Moreover, it can be seen in sample S_{49} that the ANN-based approach failed to control the output voltage and track its reference waveform. As a consequence, the UPS does not work properly due to a higher distortion in the voltage. These results could be improved using either (i) a higher sampling frequency, or (ii) a higher value of the filter capacitance C , as illustrated in sample S_{50} which represents an improvement of the result of sample S_{49} . An alternative solution to be considered to improve the performance of the controller is to increase the number of training instances, taking into account various values of C and T_s . In addition, it is observed that having a one-delay step in the input features of the neural network improves its performance to outperform that of MPC. For example, $(THD)_{ANN}$ of samples $S_{26}, S_{27}, S_{28}, S_{29}, S_{49}$ is decreased to be 3.72%, 2.39%, 4.08%, 2.35%, 3.86%, respectively.

VI. CONCLUSION

A novel control strategy using a feed-forward ANN in order to generate a high-quality sinusoidal output voltage of a three-phase inverter with an output LC filter has been successfully developed and tested, for different types of loads with various operating conditions. The output voltage of the inverter is directly controlled, without the need for the mathematical model of the inverter, considering the whole system as a black-box. In this work, MPC has been used for two main purposes: (i) generating the data required for the off-line training of the proposed ANN, and (ii) comparing its performance with the proposed ANN-based controller for linear and non-linear load conditions. Simulation results, based on fifty test samples different than those that were used at training time, show that the proposed ANN-based controller performs better than MPC, in terms of a lower THD and a fast and safe transient response, demonstrating the excellent steady and dynamic performance of the proposed ANN-based control strategy. As in any model-based control strategy, variations in the system parameters inevitably influence the performance of the ANN-based control scheme proposed in this paper.

Table II

A COMPARISON BETWEEN THE TWO PROPOSED CONTROL STRATEGIES FOR LINEAR AND NON-LINEAR LOADS UNDER DIFFERENT OPERATING CONDITIONS

Case # 1: Resistive Load as Linear Load with R							Results				
							(THD) _{ANN} [%]		(THD) _{MPC} [%] (t_{ss})		
Sample No.	R [Ω]	T_s [μ s]	L [mH]	C [μ F]	V_{dc} [V]	v_c^* [V]	(THD) _{S_1-S_{60}}	(THD) _{S_1-S_{70}}			
S_1	10	25	2.5	50	550	250	0.49	0.52	1.16 (2 ms)		
S_2	30	25	2.5	50	520	200	0.55	0.57	1.46 (5 ms)		
S_3	50	25	2.5	50	500	250	0.65	0.68	1.59 (5 ms)		
S_4	80	25	2.5	50	500	150	0.66	0.70	1.58 (10 ms)		
S_5	300	25	2.0	50	450	200	0.63	0.65	2.32 (20 ms)		
S_6	500	25	2.0	40	550	250	0.95	1.06	2.84 (35 ms)		
S_7	1 k Ω	25	3.5	40	520	200	0.72	0.70	1.51 (35 ms)		
S_8	2 M Ω	25	4.0	40	500	150	0.76	0.84	1.31 (30 ms)		
S_9	10 M Ω	25	2.0	40	500	200	0.99	0.98	2.61 (10 ms)		
S_{10}	Open Circuit		25	3.5	40	450	150	0.79	0.83		
S_{11}	15	30	2.5	50	550	250	0.72	0.74	1.75		
S_{12}	40	30	2.5	50	520	200	0.86	0.83	2.04		
S_{13}	100	30	2.5	50	500	250	0.88	1.12	2.36		
S_{14}	200	30	2.5	50	500	150	0.98	0.95	2.40		
S_{15}	300	30	2.0	50	450	200	0.96	0.99	3.33		
S_{16}	500	30	2.0	40	500	200	1.58	1.82	3.49		
S_{17}	2 k Ω	30	3.5	40	520	200	1.15	1.09	2.36		
S_{18}	1 M Ω	30	4.0	40	500	150	1.20	1.27	1.88		
S_{19}	5 M Ω	30	2	40	500	200	1.61	1.62	3.91		
S_{20}	Open Circuit		30	2.0	40	450	250	2.25	2.25		
S_{21}	20	35	2.5	50	550	250	1.11	1.21	2.67		
S_{22}	100	35	2.0	50	520	200	1.66	1.66	3.85		
S_{23}	250	35	3.5	40	500	150	2.10	2.33	2.92		
S_{24}	400	40	2.5	50	500	200	2.27	2.48	4.11		
S_{25}	500	40	4.0	45	450	200	1.50	1.89	2.91		
S_{26}	400	40	2.5	40	500	200	5.40	4.87	4.42		
S_{27}	3 k Ω	35	2.0	40	550	200	4.23	4.30	4.19		
S_{28}	3 k Ω	40	2.0	40	500	150	8.44	8.87	5.63		
S_{29}	1 M Ω	35	3.0	35	500	200	4.66	4.81	3.61		
S_{30}	Open Circuit		40	3.5	40	450	150	5.39	5.15		
Case # 2: Diode-Bridge Rectifier as Non-Linear Load with R_{NL} and C_{NL}							Results				
							(THD) _{ANN} [%]		(THD) _{MPC} [%]		
Sample No.	R_{NL} [Ω]	C_{NL} [μ F]	T_s [μ s]	L [mH]	C [μ F]	V_{dc} [V]	v_c^* [V]	(THD) _{S_1-S_{60}}	(THD) _{S_1-S_{70}}		
S_{31}	10	3000	25	2.4	50	520	200	3.97	3.97	7.44	
S_{32}	30	3000	25	3.5	50	500	200	1.99	2.10	3.80	
S_{33}	60	3000	25	2.0	50	500	250	1.97	1.98	2.76	
S_{34}	1 k Ω	3000	25	2.4	40	550	150	0.97	0.94	2.11	
S_{35}	1 k Ω	200	25	3.5	35	520	200	0.80	0.90	1.40	
S_{36}	60	100	25	4.0	40	450	150	1.36	1.30	1.64	
S_{37}	100	1000	25	2.5	30	520	250	2.22	2.47	2.98	
S_{38}	20	2000	33	3.0	50	520	200	2.94	3.10	4.57	
S_{39}	30	2000	33	3.5	40	500	200	3.77	3.32	3.69	
S_{40}	60	2000	33	2.0	50	500	250	3.15	3.31	4.08	
S_{41}	2 k Ω	3000	33	2.4	40	550	150	2.90	2.89	3.65	
S_{42}	2 k Ω	200	33	3.5	35	520	200	2.22	2.19	2.55	
S_{43}	60	100	33	4.0	40	450	150	1.69	1.74	1.97	
S_{44}	80	1000	33	4.0	35	520	250	3.47	3.60	3.66	
S_{45}	100	3000	40	3.5	50	500	200	2.04	2.22	2.92	
S_{46}	900	3000	40	3.0	40	520	250	4.32	4.30	4.65	
S_{47}	100	1000	40	4.0	50	450	200	2.73	2.70	2.84	
S_{48}	100	5000	40	4.0	45	520	250	3.71	3.79	3.63	
S_{49}	1 k Ω	3000	40	2.5	35	500	150	22.23	21.50	5.78	
S_{50}	1 k Ω	3000	40	2.5	50	500	150	2.41	2.30	4.76	

REFERENCES

- P. Cortés, G. Ortiz, J. I. Yuz, J. Rodríguez, S. Vazquez, and L. G. Franquelo, "Model predictive control of an inverter with output LC filter for UPS applications," *IEEE Transactions on Industrial Electronics*, vol. 56, no. 6, pp. 1875–1883, 2009.
- T. G. Habetler, R. Naik, and T. A. Nondahl, "Design and implementation of an inverter output LC filter used for dv/dt reduction," *IEEE Transactions on Power Electronics*, vol. 17, no. 3, pp. 327–331, 2002.
- B. K. Bose, "Power electronics and AC drives," *Englewood Cliffs, NJ, Prentice-Hall*, 1986, 416 p., 1986.
- M. P. Kazmierkowski and L. Malesani, "Current control techniques for

- three-phase voltage-source PWM converters: A survey," *IEEE Transactions on industrial electronics*, vol. 45, no. 5, pp. 691–703, 1998.
- [5] J. M. Carrasco, L. G. Franquelo, J. T. Bialasiewicz, E. Galván, R. C. PortilloGuisado, M. M. Prats, J. I. León, and N. Moreno-Alfonso, "Power-electronic systems for the grid integration of renewable energy sources: A survey," *IEEE Transactions on industrial electronics*, vol. 53, no. 4, pp. 1002–1016, 2006.
- [6] F. Blaabjerg, R. Teodorescu, M. Liserre, and A. V. Timbus, "Overview of control and grid synchronization for distributed power generation systems," *IEEE Transactions on industrial electronics*, vol. 53, no. 5, pp. 1398–1409, 2006.
- [7] J. Guerrero, L. G. De Vicuna, and J. Uceda, "Uninterruptible power supply systems provide protection," *IEEE Industrial Electronics Magazine*, vol. 1, no. 1, pp. 28–38, 2007.
- [8] J. Y. Hung, W. Gao, and J. C. Hung, "Variable structure control: A survey," *IEEE transactions on industrial electronics*, vol. 40, no. 1, pp. 2–22, 1993.
- [9] I. S. Mohamed, S. A. Zaid, M. Abu-Elyazeed, and H. M. Elsayed, "Classical methods and model predictive control of three-phase inverter with output LC filter for UPS applications," in *Control, Decision and Information Technologies (CoDIT), 2013 International Conference on*. IEEE, 2013, pp. 483–488.
- [10] D. M. Brod and D. W. Novotny, "Current control of VSI-PWM inverters," *IEEE Transactions on Industry Applications*, no. 3, pp. 562–570, 1985.
- [11] J. Jung, M. Dai, and A. Keyhani, "Optimal control of three-phase PWM inverter for UPS systems," in *IEEE Power Electronics Specialists Conference*, vol. 3, 2004, pp. 2054–2059.
- [12] I. S. Mohamed, S. A. Zaid, M. Abu-Elyazeed, and H. M. Elsayed, "Model predictive control-a simple and powerful method to control UPS inverter applications with output LC filter," in *Electronics, Communications and Photonics Conference (SIECPC), 2013 Saudi International*. IEEE, 2013, pp. 1–6.
- [13] F. Rojas, R. Kennel, R. Cardenas, R. Repenning, J. C. Clare, and M. Diaz, "A new space-vector-modulation algorithm for a three-level four-leg NPC inverter," *IEEE Transactions on Energy Conversion*, vol. 32, no. 1, pp. 23–35, 2017.
- [14] P. C. Loh, M. J. Newman, D. N. Zmood, and D. G. Holmes, "A comparative analysis of multiloop voltage regulation strategies for single and three-phase UPS systems," *IEEE Transactions on Power Electronics*, vol. 18, no. 5, pp. 1176–1185, 2003.
- [15] P. C. Loh and D. G. Holmes, "Analysis of multiloop control strategies for LC/CL/LCL-filtered voltage-source and current-source inverters," *IEEE Transactions on Industry Applications*, vol. 41, no. 2, pp. 644–654, 2005.
- [16] O. Kukrler, "Deadbeat control of a three-phase inverter with an output LC filter," *IEEE Transactions on power electronics*, vol. 11, no. 1, pp. 16–23, 1996.
- [17] P. Mattavelli, "An improved deadbeat control for UPS using disturbance observers," *IEEE Transactions on Industrial Electronics*, vol. 52, no. 1, pp. 206–212, 2005.
- [18] Y. A.-R. I. Mohamed and E. F. El-Saadany, "An improved deadbeat current control scheme with a novel adaptive self-tuning load model for a three-phase PWM voltage-source inverter," *IEEE Transactions on Industrial Electronics*, vol. 54, no. 2, pp. 747–759, 2007.
- [19] J. S. Lim, C. Park, J. Han, and Y. I. Lee, "Robust tracking control of a three-phase DC–AC inverter for UPS applications," *IEEE Transactions on Industrial Electronics*, vol. 61, no. 8, pp. 4142–4151, 2014.
- [20] M. Pichan, H. Rastegar, and M. Monfared, "Deadbeat control of the stand-alone four-leg inverter considering the effect of the neutral line inductor," *IEEE Trans. Industrial Electronics*, vol. 64, no. 4, pp. 2592–2601, 2017.
- [21] G. Escobar, P. Mattavelli, A. M. Stankovic, A. A. Valdez, and J. Leyva-Ramos, "An adaptive control for UPS to compensate unbalance and harmonic distortion using a combined capacitor/load current sensing," *IEEE Transactions on Industrial Electronics*, vol. 54, no. 2, pp. 839–847, 2007.
- [22] S. Jiang, D. Cao, Y. Li, J. Liu, and F. Z. Peng, "Low-THD, fast-transient, and cost-effective synchronous-frame repetitive controller for three-phase UPS inverters," *IEEE Transactions on Power Electronics*, vol. 27, no. 6, pp. 2994–3005, 2012.
- [23] E. Wu and P. W. Lehn, "Digital current control of a voltage source converter with active damping of LCL resonance," in *Twentieth Annual IEEE Applied Power Electronics Conference and Exposition, 2005. APEC 2005*, vol. 3. IEEE, 2005, pp. 1642–1649.
- [24] H. Komurcugil, "Rotating-sliding-line-based sliding-mode control for single-phase UPS inverters," *IEEE Transactions on Industrial Electronics*, vol. 59, no. 10, pp. 3719–3726, 2012.
- [25] S. Sabir, Q. Khan, M. Saleem, and A. Khaliq, "Robust voltage tracking control of three phase inverter with an output LC filter: A sliding mode approach," in *Emerging Technologies (ICET), 2017 13th International Conference on*. IEEE, 2017, pp. 1–5.
- [26] P. Cortés, M. P. Kazmierkowski, R. Kennel, D. E. Quevedo, and J. R. Rodriguez, "Predictive control in power electronics and drives," *IEEE Trans. Industrial Electronics*, vol. 55, no. 12, pp. 4312–4324, 2008.
- [27] V. K. Singh, R. N. Tripathi, and T. Hanamoto, "HIL co-simulation of finite set-model predictive control using FPGA for a three-phase VSI system," *Energies*, vol. 11, no. 4, p. 909, 2018.
- [28] G. Willmann, D. F. Coutinho, L. F. A. Pereira, and F. B. Líbano, "Multiple-loop H-infinity control design for uninterruptible power supplies," *IEEE Transactions on Industrial Electronics*, vol. 54, no. 3, pp. 1591–1602, 2007.
- [29] T.-S. Lee, K. Tzeng, and M. Chong, "Robust controller design for a single-phase UPS inverter using μ -synthesis," *IEE Proceedings-Electric Power Applications*, vol. 151, no. 3, pp. 334–340, 2004.
- [30] I. S. Mohamed, S. A. Zaid, H. M. Elsayed, and M. Abu-Elyazeed, "Three-phase inverter with output LC filter using predictive control for UPS applications," in *Control, Decision and Information Technologies (CoDIT), 2013 International Conference on*. IEEE, 2013, pp. 489–494.
- [31] M. Nauman and A. Hasan, "Efficient implicit model-predictive control of a three-phase inverter with an output LC filter," *IEEE Transactions on Power Electronics*, vol. 31, no. 9, pp. 6075–6078, 2016.
- [32] I. S. Mohamed, S. A. Zaid, M. Abu-Elyazeed, and H. M. Elsayed, "Implementation of model predictive control for three-phase inverter with output LC filter on eZdsp F28335 Kit using HIL simulation," *International Journal of Modelling, Identification and Control*, vol. 25, no. 4, pp. 301–312, 2016.
- [33] E. F. Camacho and C. Bordons, "Nonlinear model predictive control: An introductory review," in *Assessment and future directions of nonlinear model predictive control*. Springer, 2007, pp. 1–16.
- [34] S. Vazquez, J. Rodriguez, M. Rivera, L. G. Franquelo, and M. Norambuena, "Model predictive control for power converters and drives: Advances and trends," *IEEE Transactions on Industrial Electronics*, vol. 64, no. 2, pp. 935–947, 2017.
- [35] I. S. Mohamed, S. A. Zaid, M. Abu-Elyazeed, and H. M. Elsayed, "Improved model predictive control for three-phase inverter with output LC filter," *International Journal of Modelling, Identification and Control*, vol. 23, no. 4, pp. 371–379, 2015.
- [36] S. Mariethoz and M. Morari, "Explicit model-predictive control of a PWM inverter with an LCL filter," *IEEE Transactions on Industrial Electronics*, vol. 56, no. 2, pp. 389–399, 2009.
- [37] S. Kwak and J.-C. Park, "Switching strategy based on model predictive control of VSI to obtain high efficiency and balanced loss distribution," *IEEE Trans. Power Electron*, vol. 29, no. 9, pp. 4551–4567, 2014.
- [38] M. H. Rashid, *Power electronics handbook*. Butterworth-Heinemann, 2017.
- [39] B. Karanayil and M. F. Rahman, "Artificial neural network applications in power electronics and electric drives," in *Power Electronics Handbook (Fourth Edition)*. Elsevier, 2018, pp. 1245–1260.
- [40] M. T. Wishart and R. G. Harley, "Identification and control of induction machines using artificial neural networks," *IEEE Transactions on Industry Applications*, vol. 31, no. 3, pp. 612–619, 1995.
- [41] X. Sun, L. Chen, Z. Yang, and H. Zhu, "Speed-sensorless vector control of a bearingless induction motor with artificial neural network inverse speed observer," *IEEE/ASME Transactions on mechatronics*, vol. 18, no. 4, pp. 1357–1366, 2013.
- [42] H.-Y. Lee, J.-L. Lee, S.-O. Kwon, and S.-W. Lee, "Performance estimation of induction motor using artificial neural network," in *2018 25th International Conference on Systems, Signals and Image Processing (IWSSIP)*. IEEE, 2018, pp. 1–3.
- [43] S. M. Gadoue, D. Giaouris, and J. W. Finch, "Stator current model reference adaptive systems speed estimator for regenerating-mode low-speed operation of sensorless induction motor drives," *IET Electric Power Applications*, vol. 7, no. 7, pp. 597–606, 2013.
- [44] A. Bakhshai, J. Espinoza, G. Joos, and H. Jin, "A combined artificial neural network and DSP approach to the implementation of space vector modulation techniques," in *Industry Applications Conference, 1996. Thirty-First IAS Annual Meeting, IAS'96., Conference Record of the 1996 IEEE*, vol. 2. IEEE, 1996, pp. 934–940.
- [45] J. O. Pinto, B. K. Bose, L. B. Da Silva, and M. P. Kazmierkowski, "A neural-network-based space-vector PWM controller for voltage-fed inverter induction motor drive," *IEEE Transactions on Industry Applications*, vol. 36, no. 6, pp. 1628–1636, 2000.
- [46] E. Karatepe, T. Hiyama *et al.*, "Artificial neural network-polar coordinated fuzzy controller based maximum power point tracking control

- under partially shaded conditions," *IET Renewable Power Generation*, vol. 3, no. 2, pp. 239–253, 2009.
- [47] M. P. Akter, S. Mekhilef, N. M. L. Tan, and H. Akagi, "Modified model predictive control of a bidirectional AC–DC converter based on lyapunov function for energy storage systems," *IEEE Transactions on Industrial Electronics*, vol. 63, no. 2, pp. 704–715, 2016.
- [48] M. F. Møller, "A scaled conjugate gradient algorithm for fast supervised learning," *Neural networks*, vol. 6, no. 4, pp. 525–533, 1993.
- [49] R. Fletcher, *Practical methods of optimization*. John Wiley & Sons, Ltd, 2000, second edition.